



Research paper

Resveratrol derivatives: Synthesis and their biological activities

Laura Grau, Richard Soucek, M. Dolors Pujol*

Laboratori de Química Farmacèutica, Facultat de Farmàcia i Ciències de l'Alimentació, Universitat de Barcelona, Av. Joan XXIII, 27-31, E-08028, Barcelona, Spain



ARTICLE INFO

Keywords:

Resveratrol
 Stilbene
 Cyclic analogues
 Antitumor
 Cytotoxicity
 KRas
 Prodrug

ABSTRACT

Resveratrol, a natural compound known especially for its antioxidant properties and protective action, opens the door for both it and its structural derivatives to be considered not only as chemopreventive but also as cancer chemotherapeutic agents. Due to the pharmacokinetic problems of *resveratrol* that demonstrate its poor bioavailability, the study of new derivatives is of interest. Thus, in this work (*E*)-stilbenes derived directly from *resveratrol* and other cyclic analogues containing the benzofuran or indole nucleus have been synthesized. The synthesized compounds have been evaluated for their ability to affect tumor growth in vitro. Compounds **2**, **3**, **4** and **5** have shown cytotoxicity in human colon cancer (HT-29) and human pancreatic adenocarcinoma cells (MIA PaCa-2) higher than those of (*E*)-*resveratrol*. The indolic derivative **13**, a cyclic analog of *resveratrol*, has shown in vitro cytotoxic activity 8 times higher than *resveratrol* against HT-29 cancer cells. The cyclic derivatives **8**, **9** and **12** showed a high inhibition of cell growth in HCT-116 (KRas mutant) at 20 μ M, while **13** shows moderate antiangiogenesis activity at 10 μ M.

1. Introduction

Pharmaceutical studies suggested that the polyphenol *resveratrol* (3,4',5-trihydroxy-*trans*-stilbene) present in some plants is one of the main wine-red grape components that protect from vascular, neurodegenerative diseases, atherosclerosis, oxidative stress and certain tumors due to antioxidant properties [1–3]. The ability of *resveratrol* to prevent the occurrence of carcinomas was related to the inhibition of tumor cell cycle and induction of tumor cell death [4]. *Resveratrol*, like other natural products, can act on different biological targets and present different biological effects and therefore is considered a multi-target drug.

Resveratrol exhibits poor solubility in water and also low oral bioavailability. Complexation with cyclodextrins or the formation of salts improve the aqueous solubility but the bioavailability does not increase [5].

In addition, *resveratrol* has a very short half-life (about 14 min when it was administered intravenously) due to its rapid metabolism. The presence of free hydroxyl groups facilitates conjugation with glucuronic acid and sulphatation via PAPS (phosphoadenosyl phosphosulfate) [6].

The study of *resveratrol* is on the rise as indicated by the 34,144 references and 2,833,781 bibliographic citations in SciFinder (July 2022), of which more than 80% are from the last 5 years. Although the clinical benefits of *resveratrol* have not been sufficiently demonstrated,

the vast majority of publications refer to studies with prospective therapeutic applications.

Resveratrol is a stilbene that contains 2 hydroxyl groups on one of the phenyls and another hydroxyl group on the second benzene ring. Despite the fact that *resveratrol* and its analogues are normally in the *E*-configuration (^1H NMR analysis $J = 16.0\text{--}18.0$ Hz, ethene protons), both phenyl groups linked through an ethylene unit can give rise to the *Z* and *E* configurations.

Recently in the field of cancer, *resveratrol* has demonstrated its antimutagenic and phase II inducing capacity of hepatic enzymes detoxifying carcinogens (cytochrome P450 enzymes (CYPs)) [7]. It has also been seen that it stimulates apoptosis or programmed cell death of tumor cells, thus helping to reduce tumor growth [8]. According to the results of scientific studies, the P53 tumor suppressor protein could be considered the target for the apoptosis process since it would involve different phosphorylation enzymes and Bcl proteins [9]. In other trials, *resveratrol* has been shown to activate the suppressor gene Rad 9 which induces the death of tumor cells. In this specific case, *resveratrol* has shown a reduction in lung and breast cancer at micromolar concentration in vitro and also in vivo test [10]. Pradhan and col [11]. report that *resveratrol* inhibits metastasis and angiogenesis by reducing inflammatory cytokines in oral cancer cells by attacking primarily tumor-related macrophages. In short, it can be said that *resveratrol* affects all three phases of cancer development, initiation, promotion and progression,

* Corresponding author.

E-mail addresses: lauragrauvals@gmail.com (L. Grau), soucek.richard@gmail.com (R. Soucek), mdpujol@ub.edu (M.D. Pujol).<https://doi.org/10.1016/j.ejmech.2022.114962>

Received 6 September 2022; Received in revised form 11 November 2022; Accepted 23 November 2022

Available online 26 November 2022

0223-5234/© 2023 The Authors.

Published by Elsevier Masson SAS. This is an open access article under the CC BY license (<http://creativecommons.org/licenses/by/4.0/>).

and also suppresses final steps such as angiogenesis and metastasis.

Currently, *resveratrol* continues to be of interest due to its multiple properties of therapeutic interest, especially its antitumor capacity. Previously, and due to its antioxidant nature, *resveratrol* was considered preventive against the development of cancer, today, there are research results that allow us to recognize its dose-dependent cytotoxic properties and can be considered chemopreventive and therapeutic agent [12]. Because of its antitumor properties and its low toxicity even at high doses, *resveratrol* constitutes a good head for the design of new compounds.

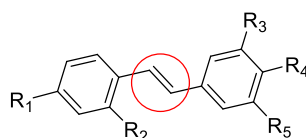
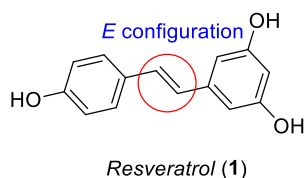
Resveratrol has been well studied and its biological properties and even mechanisms of action are known, but there is virtually no information on other stilbenoids. On the one hand, and as in resultant the low bioavailability of *resveratrol* attributable to phenolic functions, we proposed the preparation of derivatives with protected hydroxyl groups or without these polar groups to improve activity as prodrugs by comparing it with to *resveratrol* itself (Fig. 1).

To improve bioavailability and its cytotoxic capacity, in this work, *resveratrol* derivatives have been prepared by alkylation of hydroxyl groups (compounds 2, 4 and 5) or acylation (compounds 6 and 7). Cyclic analogues of *resveratrol* have also been prepared, and their preparation and biological activities will be discussed. Compounds 2 and 4 had already been reported previously [bibliographic references 1e, 3b, 4c] but there are few data about them and here they were important to be able to make a comparative study of the biological activities.

In the design of new compounds from a model, in our case *resveratrol*, the formation of rings constitutes a classic approach to modulative pharmacomodulation. The preparation of cyclic analogues of *resveratrol* leads to an increase in the rigidity of the structure and constitutes an interesting method for the determination of the pharmacophore group of structures with a clear profile of biological activity. We focused on the synthesis of new structural *resveratrol* analogues replacing the central double bond by an unsaturated ring furan or pyrrole. In this work, the preparation of derivatives of the 2-arylbenzofuran type (compounds 8–11) by the introduction of an oxygen atom or of derivatives that contain the nucleus of 2-arylindoles that differ from *resveratrol* by the incorporation of an –NH– group that allows the formation of the heterocyclic ring (compounds 12–15) (Fig. 2) was carried out.

According to bibliographic data, the role of *resveratrol* against the Kras protein, as well as its antiangiogenesis properties are unknown. For this reason, our interest would be to determine the in vitro antitumor activity in colon cell lines as well as to determine the participation of Kras in the cytotoxic capacity of *resveratrol*.

Kras inhibition and angiogenesis studies have been carried out on the compounds selected and accepted by the Eli Lilly Laboratories OIDDs program (Open Innovation Drug Discovery Program). The OIDDs platform selected some of the compounds prepared in this work according to their structure to carry out in vitro biological tests against specific and concrete targets. This being the reason why the activity of each of the compounds against the different targets mentioned has not been indicated.



2. $R_1 = R_2 = R_3 = R_4 = R_5 = \text{OCH}_3$
3. $R_1 = R_2 = R_3 = R_4 = R_5 = \text{OH}$
4. $R_1 = R_3 = R_5 = \text{OCH}_3$; $R_2 = R_4 = \text{H}$
5. $R_1 = R_3 = R_5 = \text{OCH}_2\text{CH}_2\text{OH}$; $R_2 = R_4 = \text{H}$
6. $R_1 = R_3 = R_5 = \text{O-CO-C}(\text{CH}_3)_3$; $R_2 = R_4 = \text{H}$
7. $R_1 = R_3 = R_5 = \text{O-CO-(CH}_2)_{10}\text{CH}_3$; $R_2 = R_4 = \text{H}$

Fig. 1. *Resveratrol* derivatives.

2. Results and discussion

2.1. Chemistry

The synthetic routes for the preparation of *resveratrol* derivatives 2–7, 8–15 are shown in Schemes 1–4.

The condensation between 2,4-dimethoxybenzaldehyde (16) and 3,4,5-trimethoxybenzaldehyde (17) under McMurry reaction conditions [13] led to the *trans* stilbene 2 in moderate yield (Scheme 1). The five methoxy groups of the stilbene 2 were then cleaved with BBr_3 to afford the pentahydroxystilbene 3 in high yield.

The polyalkylation of *resveratrol* with an excess of alkylating agents in basic medium allows access to alkylated derivatives such as 4 [14] and 5. Methylation using methyl iodide leads to 4 with quantitative yields while the reaction with 2-bromoethanol leads to a mixture of monoalkylated, dialkylated compounds and the trialkylated desired compound 7 being a minority (Scheme 2). Compounds 6 and 7 were prepared by acylation of *resveratrol*. Treatment of *resveratrol* with an excess of pivaloyl chloride makes it possible to obtain the triacylated derivative 6 with a yield of 66%. X-ray diffraction studies confirmed the structure proposed for derivative 6 and also confirms the proposed configuration *E*. (Fig. 3). In the same way, the treatment of *resveratrol* with lauroyl chloride in the presence of base allows access to the triacylated derivative 7 with a yield of 52% (Scheme 2).

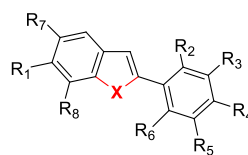
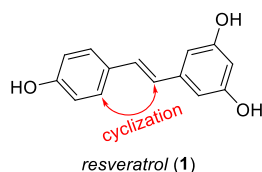
A multistep and metal-free approach for the preparation of *resveratrol* analogues was proposed. Firstly, a condensation of the corresponding aldehyde 18 with the appropriate phenylacetic acid (19 or 20) under Perkin-type conditions using Ac_2O and Et_3N led to the intermediate arylcoumarins (21–22) in moderate yield. The corresponding lactones (21–22) were separately hydrolyzed and involved in an intramolecular cyclization reaction with 2 N HCl to afford the benzofurans (8 or 10) in moderate yield. The methoxyl groups of 8 were cleaved by treatment with BBr_3 at 0 °C affording 9 in satisfactory yield (Scheme 3). This process through the opening of the coumarin ring followed by decarboxylation in the presence of acid has a high *trans* selectivity and uses environmentally friendly conditions.

The 2-bromo-1-(substituted phenyl)ethanone (26–28) and the corresponding aniline (23–25) were involved in a modified Bischler-Möhlau reaction [15] in *N,N*-dimethylaniline yielding the 2-arylindoles 12, 14 and 15 in moderate yield. Deprotection of the benzyl group of 12 in a catalytic hydrogenation by H_2 , Pd/C in EtOAc and MeOH led to 13 in satisfactory yield (Scheme 4).

2.2. Biological results

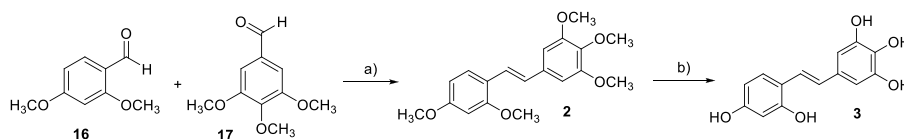
2.2.1. Determination cytotoxic activity

The in vitro cell proliferation of *resveratrol* (1) and synthetic *resveratrol* derivatives 2–7 was evaluated against two cancer cell lines, HT-29 (human colon adenocarcinoma) and MIA PaCa-2 (human pancreatic adenocarcinoma cells) by standard MTT assay (see the experimental section) and cytotoxicity values as IC_{50} are shown in Table 1.

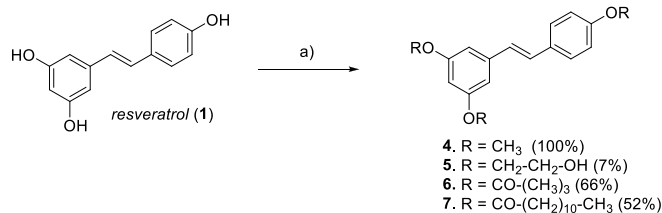


8. X = O, R₁ = OH, R₂ = R₆ = R₇ = R₈ = H, R₃ = R₄ = R₅ = OCH₃
9. X = O, R₁ = OH, R₂ = R₆ = R₇ = R₈ = H, R₃ = R₄ = R₅ = OH
10. X = O, R₁ = OH, R₂ = R₄ = R₆ = R₇ = R₈ = H, R₃ = R₅ = OCH₃
11. X = O, R₁ = OH, R₂ = R₄ = R₆ = R₇ = R₈ = H, R₃ = R₅ = OH
12. X = NH, R₁ = OBn, R₂ = R₅ = OCH₃, R₃ = R₄ = R₆ = R₇ = R₈ = H
13. X = NH, R₁ = OH, R₂ = R₅ = OCH₃, R₃ = R₄ = R₆ = R₇ = R₈ = H
14. X = NH, R₁ = R₂ = R₃ = R₅ = R₆ = R₇ = H, R₄ = R₇ = R₈ = OCH₃
15. X = NH, R₁ = R₂ = R₃ = R₅ = R₆ = H, R₄ = OCH₃, R₇ = R₈ = CH₃

Fig. 2. Resveratrol derivatives.



Scheme 1. Reagents and conditions: a) Zn (5 eq), TiCl₄ (2.5 eq), THF (30 mL), reflux, 72 h, 38%. b) BBr₃ (10 eq), 0 °C, 30 min, 98%.



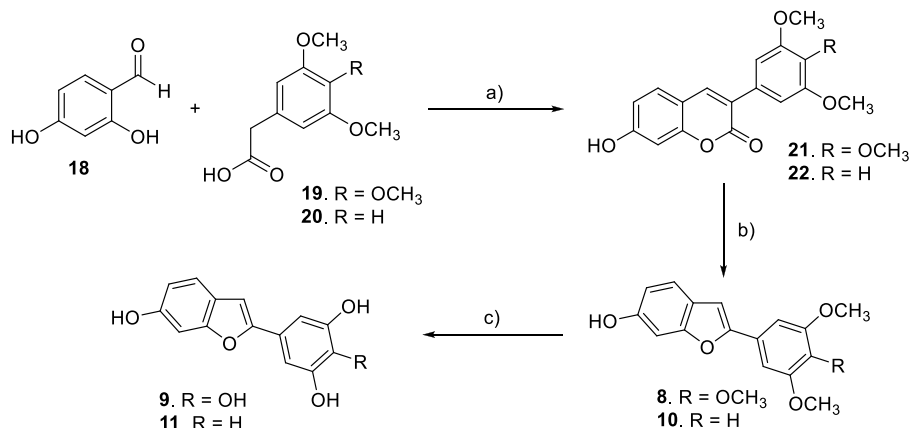
Scheme 2. Reagents and conditions: For 4: a) CH₃I (excess), K₂CO₃ (6 eq), DMF, rt, 3 days. For 5: a) Br-(CH₂)₂-OH (10 eq), K₂CO₃ (6 eq), acetone-ethanol, rt. For 6: a) (CH₃)₃-CO-Cl (6 eq), Et₃N (6 eq), acetone, rt. For 7: a) CH₃-(CH₂)₁₀-CO-Cl (6 eq), Et₃N (6 eq), acetone, rt.

The tested compounds show differences in activities with respect to *resveratrol* against the two tumor cell lines. The pentahydroxylated compound 3 shows activity comparable to that of *resveratrol* for HT-29 cells and a lower IC₅₀ value for MIA PaCa-2 cells (IC₅₀ = 96 ± 5 μM). Trialcohol 5 surprisingly show greater cytotoxicity than expected in both types of cell lines. Regarding tumor cells HT-29 show a cytotoxicity 3 times higher than *resveratrol* (IC₅₀ = 23 ± 2 μM). Polyphenol 3 has cytotoxic activity comparable to *resveratrol* in the HT-29 cell line and higher in pancreatic cancer cells. The 3,4,5-trimethoxyphenol group of

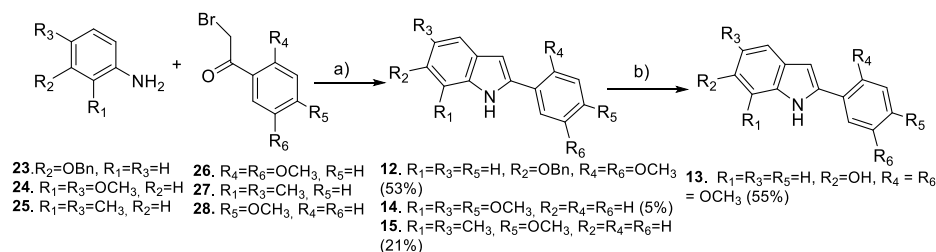
compound 3 can establish intramolecular hydrogen bonds that provide greater solubility in organic solvents than *resveratrol* favoring the passage of membranes. Polyphenol 3 and trialcohol 5 show practically the same log P values, however the IC₅₀ values are different, being markedly 5 more active than polyphenol 3 markedly in HT-29 cells.

Compound 2 shows the strongest cytotoxicity against colon carcinoma (HT-29) and pancreatic carcinoma (MIA PaCa-2) cells lines with IC₅₀ values of 12 ± 3 and 28 ± 4 μM respectively, being six and five times more active than *resveratrol* in the respective cell lines. The methoxylated-*resveratrol* 4 also shows significant cytotoxicity 5- and 4-fold higher than *resveratrol* on HT-29 and MIA PaCa-2 cells, respectively. The pivaloyl ester 6, in these tests, showed a higher activity than that of *resveratrol* in both cell lines, showing that the triester has not been hydrolyzed to *resveratrol* (1) as might be expected. Triester 7, a more lipophilic compound, has less activity than *resveratrol* (1). The decrease in activity can be attributed to the low solubility and high stability of this derivative. Finally indicate that there is no direct relationship between lipophilicity and cytotoxicity of the seven compounds evaluated. But the results indicate that the compounds with logP between 2.29 and 3.85 are the ones that present greater cytotoxicity in vitro in HT-29 and MIA PaCa-2 cells lines.

Regarding the cyclic analogues of *resveratrol*, 2-arylindole 13 turns out to be the most active against HT-29 colon cancer tumor cells, this



Scheme 3. Reagents and conditions: a) Et₃N (5 eq), Ac₂O, reflux, 3 h, 47%. b) EtOH/HCl (2 N) 8:2, reflux, 16 h, 29%. c) BBr₃ (20 eq), DCM, rt, 3 h, 51%.



Scheme 4. Reagents and conditions: a) DMA, 165 °C, 1 h. b) H₂, Pd/C, EtOAc, MeOH, rt, 16 h, 55%.

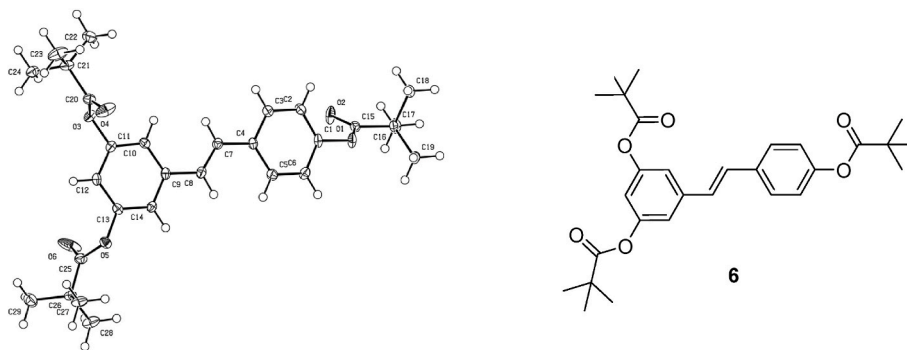


Fig. 3. ORTEP (A) and the structure of 6.

Table 1

Cytotoxicity of *resveratrol* (1) and analogues 2–7.

Compound	Log P	IC ₅₀ (μM)	
		HT-29	MIA PaCa-2
2	3.59	12 ± 3	28 ± 4
3	2.28	78 ± 8	96 ± 5
4	3.85	16 ± 3	35 ± 4
5	2.29	23 ± 2	79 ± 5
6	8.76	56 ± 4	39 ± 7
7	>11.2	134 ± 8	198 ± 9
<i>Resveratrol</i> (1)	3.06	78 ± 4	132 ± 6

IC₅₀: Concentration that causes 50% inhibition in an MTT assay. Data are expressed as the mean ± SE from the dose-response curves of three independent experiments. P < 0.005, significant difference compared to the control. Log P (Partition Coefficient) was determined using ChemDraw 20.0.

compound shows a 6-hydroxyl group and a 2,5-dimethoxyphenyl group in the carbon -two. The rest of the compounds of the indole series (compounds 12, 14 and 15) show a very weak cytotoxic activity. It should be noted that only compound 13 shows a hydroxyl group specifically in position 6, the rest do not contain free hydroxyl groups in any other position (Table 2). Derivative 12, a benzylated analog of 13, has a cytotoxic activity 24 times lower than that of compound 13, confirming the importance of having a hydroxyl group in the structure.

Regarding the cyclic derivatives with a benzofuran nucleus, the four compounds of the miniseries (compounds 8–11) show greater activity than the indolic derivatives with the exception of compound 13. It should be noted that all these compounds have a hydroxyl group at C-6. In addition, the two most active compounds 8 and 10 also show 2 methoxyl groups as substituents on the phenyl group at the position of the heterocyclic nucleus, like derivative 13, although in other positions. As far as lipophilicity is concerned, the results indicate that the most lipophilic compounds (compounds 12 and 15) are those with the least cytotoxic capacity against HT-29 cells *in vitro*. These results are of interest for the design of new compounds in order to be able to optimize the results. Thus, within these cyclic derivatives of resveratrol, compound 8 can be considered a hit for the design of new compounds with

Table 2

Cytotoxicity of *resveratrol* (1) and cyclic analogues 8–15.

Compound	Log P	IC ₅₀ (μM)
		HT-29
8	2.61	14 ± 3
9	1.82	56 ± 4
10	2.74	19 ± 1
11	2.21	73 ± 2
12	5.15	239 ± 5
13	2.66	10 ± 2
14	2.93	211 ± 4
15	4.15	331 ± 3
<i>Resveratrol</i> (1)	3.06	78 ± 4

IC₅₀: Concentration that causes 50% inhibition in an MTT assay. Data are expressed as the mean ± SE from the dose-response curves of three independent experiments. P < 0.005, significant difference compared to the control. Log P (Partition Coefficient) was determined using ChemDraw 20.0.

potential activity against HT-29 colon cancer cells.

2.3. Determination of KRas activity

The substituted benzofurans 8–9 and indoles 12–13 were selected by the Eli Lilly Laboratory (Indianapolis, USA) and submitted for biological testing to evaluate their therapeutical activities.

The KRas synthetic lethal phenotypic module measures survival in colon cancer cells with mutations that activate both Wnt and KRas oncogene signaling, based on the effect of synthetic lethality, to identify compounds that inhibit colon cancer formation with KRas mutations [16]. The KRas mutation is detected in 35–42% of colon carcinoma and also in advanced adenomas [17]. Many scientific works emphasize that the development of colon cancer is due to an activation of the two pathways, KRas and Wnt. It has also been shown that the two previous pathways can participate in the regulation of vascular endothelial growth factor [18,19].

Compounds 8, 9, 12 and 13 have been tested in *in vitro* assays and 8, 9 and 12 show significant growth inhibition of human colorectal HCT116 cancer cells (KRas mutant) at 20 μM (Table 3).

According to the results, the four tested *resveratrol* analogues have a low to moderate K-Ras activity depending on the cancer cell line. The benzofurans **8** and **9** have a moderate K-Ras activity on the RKO KRas SL cell line and low or no activity on the other cancer cell lines (Table 3). The trihydroxyphenyl group of **9** does not bring a better K-Ras activity compared to the trimethoxyphenyl group of **8**, which suggests that neither the polarity nor the geometry of this moiety are decisive for its K-Ras activity. The arylindole **12** has an interesting K-Ras activity on HCT KRas SL, RKO KRasSL and SNU-C1 KRas SL cell lines. Compound **13** has a moderate K-Ras activity on Colo 320 KRas SL and SNU-C1 KRas SL. The difference of activity of **12** and **13** suggests that the benzyl group is important for the selectivity of these compounds between the different colon cell lines. These results show that the benzyl group produces an increase in lipophilicity and can modify behavior. The substituted indole **12** has nearly the same K-Ras activity on RKO KRas SL at high and low concentration, which suggests that its activity is not dose-dependent. *Resveratrol* tested under these conditions shows inhibitions of less than 15% (Table 3). No correlation was found between lipophilicity and the biological activity exhibited by these structural derivatives of *resveratrol*.

2.4. Determination of anti-angiogenesis activity

It appears that the process of angiogenesis is independent of the KRas gene status. But the process of tumor angiogenesis as well as the role of KRas arouse great interest in attempts to improve the treatment of colorectal cancer. The vascular endothelial growth factor (VEGF) pathway is critical for the regulation of angiogenesis, and research has focused on developing agents that selectively inhibit it [20]. So, both the KRas protein and VEGF are considered good targets for the development of chemotherapeutic agents (Table 4).

Results of the four cyclic *resveratrol* analogues showed that only **13** has a significant anti-angiogenesis activity. None of them have a significant osteoporosis activity (Table 4).

According to the results obtained, it is clear that free hydroxyl groups would not be necessary to show activity on KRas-Wnt, since **8** and **9** show very similar results.

The K-Ras, antiangiogenesis and antiosteoporosis activity of these *resveratrol* analogues were compared with the activities shown by *resveratrol* (**1**) under the same conditions tested, which did not show activity in any of these targets.

Within the biological study carried out by Eli Lilly laboratories, compounds **8**, **9**, **12** and **13** were also tested against the target HNNMT and it should be noted that only compound **9** showed a significant inhibition of a cancer-associated metabolic to enzyme nicotinamide-*N*-methyltransferase (HNNMT) (Inhibition of HNNMT = 77% at 10 μ M, results not indicated in the Tables). This protein is a metabolic enzyme that catalyzes the transfer of methyl groups using S-adenosyl-L-

methionine and its overexpression is associated with resistance to chemotherapy and radiotherapy and tumor aggressiveness [21].

2.5. Determination of CGRP antagonist activity

On the other hand, calcitonin gene-related peptide (CGRP) is a multifunctional neuropeptide produced by alternative splicing of the calcitonin gene [22]. CGRP is widely distributed in the nervous system, particularly in anatomical structures possibly involved in the pathophysiology of migraine, including the trigeminus-vascular system. Over the last two decades, the body of clinical and basic science studies have established the pivotal role of CGRP in migraine [23]. CGRP increases sensitivity to sensory stimuli at multiple levels, both in the central nervous and in the peripheral systems. In the brain, the wide distribution of CGRP and its receptors indicates several possible sites in which this peptide acts as a neuromodulator. Currently, CGRP has emerged as a therapeutic target for new treatments of migraine. This peptide is elevated in migraine and its antagonists have an application for migraine attacks.

The benzofurans **8** and **9** exhibit CGRP inhibitory activities at concentrations of 30 μ M, without showing a significant difference between them. When it decreases to 12.5 μ M (secondary test) only the analog with the trimethoxyphenyl group **8** shows a slight inhibitory activity, so that this nucleus is favored over trihydroxyphenyl nuclei, which could be attributed to the increase in lipophilicity (Table 5). Under these conditions, cyclic derivatives **8** and **9** show better results than *resveratrol*.

2.6. Determination of inhibition of tau protein

Tau protein is abundant in the central nervous system, while it is not as common in other parts of the body. It is mostly expressed in neurons, but has also been detected in astrocytes and oligodendrocytes. Tau belongs to the group of microtubule-associated proteins (MAPs) and their isomeric forms are the result of the alternative splicing of a single gene called MAPT (Microtubule Associated Protein Tau). The function of the Tau protein is to stabilize the microtubules present in the cells [24,25].

Los benzofurans **8** and **9** showed an inhibition of 58 and 55% of Tau protein respectively at concentrations of 40 μ M (Table 6). As in the previous case, there is no difference between the phenolic compound and the methylated derivative with respect to the inhibition of the Tau protein. Tau are very rare prionoid microtubular proteins outside the central nervous system.

Their main function is to stabilize the axonal microtubules through interaction with tubulin. However, when kinesin adheres to tau protein strips, the motor tends to come off the microtubule completely. In this way, tau protein helps regulate the balance of nerve cell trafficking,

Table 3
KRas inhibition by *resveratrol* **1** and analogues **8**, **9**, **12** and **13**.

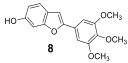
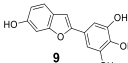
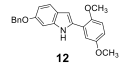
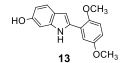
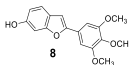
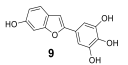
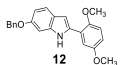
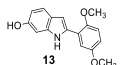
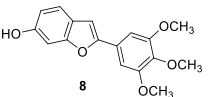
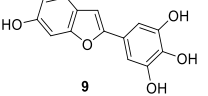
Assays		Compounds				RSV	
							
K-Ras Wnt Synthetic Lethal	HCT KRasSL	%Inh 0.2 μ M	0	15.6	0	0	0
		%Inh 2 μ M	0.5	0.5	6.9	0	0
	RKO KRasSL	%Inh 20 μ M	0	0	48.9	6.3	0
		%Inh 0.2 μ M	0	2.7	77.3	9.4	2.3
	HCT-116	%Inh 2 μ M	6.3	33	45.6	0	7.0
		%Inh 20 μ M	87.4	85.9	89.7	0	14.6
	Colo 320	%Inh 0.2 μ M	0	0	0	0	0
		%Inh 2 μ M	4.4	0	0	0	0
	KRasSL	%Inh 20 μ M	0	0	0	55.3	0
		%Inh 0.2 μ M	8.7	5.8	7.4	0	6.6
	SNU-C1	%Inh 2 μ M	8.7	3.1	13.9	0	8.0
		%Inh 20 μ M	14.9	11.2	44.5	30.3	11.2
		Log P	2.61	1.82	4.66	2.66	3.06

Table 4
Antiangiogenesis activity of the *resveratrol* (**1**) and analogues **8**, **9**, **12** and **13**.

Assays		Compounds					RSV
							
Anti-angiogenesis	Angio Tube Area	%Inh 2 μM	0	0	0	45.2	0
		%Inh 10 μM	15.7	13.8	0	73.7	2
		IC ₅₀	N.A.	N.A.	N.A.	>10 μM	N.A.
	Angio Nuc Area	IC ₅₀	N.A.	N.A.	N.A.	>10 μM	N.A.
Wnt Pathway	Osteo bCat	%Stim 2 μM	2	0	14.1	0.7	0
		%Stim 10 μM	10.2	5.5	5.4	18.1	0

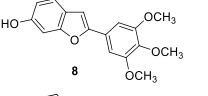
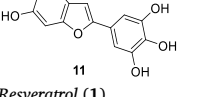
Angiogenesis nuclear area, β-catenin osteoporosis and angiogenesis tube area (tracheal tube area). N.A. not applicable.

Table 5
CGRP receptor antagonist activity of compounds **8** and **9**.

	CGRP Receptor Antagonist			
	Primary SP	Primary CRC		Secondary
	hCGRP1 cAMP	hCGRP1 cAMP	Kb (μM)	hCGRP CHO FB
	%Inhib @ 30 μM	IC ₅₀ (μM)		%Inhib @ 12,5 μM
	54.2	2.413	776.1466	-16.3 29.8
	59.9	2.772	891.7323	-27.6 4.0
<i>Resveratrol</i> (1)	2.3	-	>1000	-

CHO: ovarian cancer cells. SP: Single Point. CRC: Concentration Response Curve.

Table 6
Inhibition of Tau protein of compounds **8** and **9**.

Compounds	Tau protein
	Primary SP
	hTau_mRuby2 Huh7 TT Inh. SP
	%Inh @ 40 μM
	57.98
	55.26
<i>Resveratrol</i> (1)	21.34

Huh7: human hepatocyte cell lines. SP: Single Point.

which may explain why tau disorders are associated with neurodegenerative disorders such as Alzheimer and Parkinson diseases. *Resveratrol* has little activity against the Tau protein.

We do not have bioavailability results of the synthesized compounds, but it is expected that those compounds that have totally or partially methoxylated phenol groups have better bioavailability than *resveratrol*.

3. Conclusion

New *resveratrol* analogues **2–7** and **8–15** were successfully prepared. Arylbenzofurans were prepared by condensation of the aldehyde with the appropriate phenylacetic acid under Perkin-reaction conditions and

subsequent hydrolysis and cyclization of the intermediate lactone, while indole derivatives were synthesized from 2-bromoarylethanone and the corresponding aniline under Bischler-Möhlau reaction conditions. The pharmacokinetic problems that condition the poor bioavailability of *resveratrol* limit its possible applications. For this reason, the study of analogous compounds that maintain a broad profile of therapeutic activities is of interest. The methylated derivatives (**2**, **4**), the triol **5** or the triester **6** have shown a significant decrease in the growth of human colon cancer tumor cells (HT-29) and also of the pancreatic carcinoma cell line (MIA PaCa-2) and much higher than that caused by (*E*)-*resveratrol*. The benzofuran derivatives **8**, **9** and the indolic derivative **12** have shown marked cytotoxic activity against HCT116 (Kras mutant) at 20 μM in vitro. While **13** showed a high antiangiogenesis character at 10 mM, benzofurans **8** and **9** exhibited inhibition of CGRP and Tau protein. The activity results obtained show that compounds **8** and **9** show activity against different biological targets and could be considered potential candidates in cancer drug discovery for study and optimization. With the results that we have among the cyclic analogues derived from *resveratrol*, arylbenzofuran **8** presents a multitarget profile and could be considered a hit for the design of new compounds with potential activity against colon cancer.

4. Experimental section

4.1. General chemical synthesis

Melting points (mp) were obtained on an MFB-595010M Gallenkamp apparatus with digital thermometer in open capillary tubes and are reported without correction. IR spectra were obtained using FTIR Perkin-Elmer 1600 Infrared Spectrophotometer. ¹H and ¹³C NMR spectra were recorded on a Bruker or Varian Gemini-300 and 400 (75.5 and 100.6 MHz respectively). Chemical shifts are reported in parts per million (ppm) relative to the central peak of the solvent: CDCl₃ (δ, 7.26 (¹H) and 77.16 (¹³C)), CD₃OD (δ, 3.31 (H) and 49.45 (C)), DMSO-*d*₆ (δ, 2.49 (H) and 39.51 (C)) as internal standards. The following abbreviations are used for the proton spectra multiplicities: s, singlet, d, doublet, t, triplet, q, quadruplet, m, multiplet. Coupling constants (*J*) are reported in Hertz (Hz). The reactions were monitored by thin-layer chromatography (TLC) analysis using silica gel (60 F254, Merck) plates. Compounds were visualized by UV irradiation. Column chromatography was performed with silica gel 60 (230–400 mesh, 0.040–0.063 mm) and automatic column chromatography was performed with a CombiFlash R_f system with UV-vis (PN 68-5230-008) detector and RediSep R_f 4 and 12 g silica gel column. Elemental analysis C, H, N were realized at Serveis Científico-Tècnics UB on organic analyzer Thermo EA Flash 2000 (Thermo Scientific Apparatus). High-resolution mass spectra (HRMS) were performed on a LC/MSD-TOF (2006) (Agilent technologies) by the «Section of spectrometry of masses» at the University of Barcelona. All reagents were of high quality or were purified before use. Organic solvents were of analytical grade or were purified by standard procedures.

(*E*)-[1-(3,4,5-Trimethoxyphenyl)-2-(2,4-dimethoxyphenyl)]

ethene (2). Zn (0.8 g, 12 mmol) and anhydrous THF (30 mL) were put in a three-neck round-bottom flask under argon. The reaction was cooled to 0 °C and TiCl₄ (0.65 mL, 6 mmol) was added portion wise. The reaction mixture was allowed to warm up at rt for 30 min and refluxed under stirring for 2.5 h. The solution was cooled down to 0 °C, then 3,4,5-trimethoxybenzaldehyde (471 mg, 2.4 mmol) and 2,4-dimethoxybenzaldehyde (400 mg, 2.4 mmol) were dissolved in anhydrous THF (30 mL) in a flame-dried round-bottom flask and added to the solution. The resulting mixture was heated to reflux under stirring for 3 days and TLC of the crude reaction (EtOAc/hexane, 1:1) indicated formation of a major compound (R_f 0.65) and complete consumption of starting material (R_f 0.85, R_f 0.75). The crude mixture was quenched with NaHCO₃ (25 mL of a 10% aqueous solution) and extracted with CH₂Cl₂ (3 × 20 mL). The combined organic phases were dried (Na₂SO₄) filtered and concentrated *in vacuo*. The residue was purified by silica gel flash column chromatography (hexane/EtOAc 7:3) to afford (*E*)-[1-(3,4,5-trimethoxyphenyl)-2-(2',4')dimethoxyphenyl]ethene (2) (302 mg, 38% yield) as a white solid. R_f = 0.75 (hexane/EtOAc 1:1). mp: 115–117 °C (hexane/EtOAc) [20]. IR (film) ν cm⁻¹: 2933 (Ar–H), 2836 (=C–H), 1205 (Ar–O), 1128 (C–O). NMR ¹H (Acetone-d₆, 300 MHz) δ (ppm): 3.84 (s, 3H, CH₃–O), 3.88 (s, 3H, CH₃–O), 3.88 (s, 3H, CH₃–O), 3.91 (s, 6H, CH, CH₃–O x 2), 6.49 (d, *J* = 2.4 Hz, 1H, H-3), 6.51 (dd, *J* = 2.4 Hz, *J* = 8.4 Hz, 1H, H-5), 6.73 (s, 2H, H-2', H-6'), 6.94 (d, *J* = 16.4 Hz, 1H, Ar–CH=CH–Ar), 7.28 (d, *J* = 16.4 Hz, 1H, Ar–CH=CH–Ar), 7.49 (d, *J* = 8.4 Hz, 1H, H-6). NMR ¹³C (Acetone-d₆, 75.5 MHz) δ (ppm): 55.8 (CH₃, OCH₃ (x 2)), 56.4 (CH₃, OCH₃ (x 2)), 61.2 (CH₃, OCH₃), 98.8 (CH, C-3), 103.7 (CH, C-2', C-6'), 105.3 (CH, C-5), 119.7 (C-1), 123.2 (CH, Ar–CH=CH–Ar), 127.3 (CH, Ar–CH=CH–Ar), 127.6 (CH, C-6), 134.5 (C-1'), 137.8 (C-4'), 153.6 (C-3', C-5'), 158.3 (C-2), 160.9 (C-4).

3,4,5,2',4'-Pentahydroxystyrene (3). (*E*)-[1-(3,4,5-trimethoxyphenyl)-2-(2',4')dimethoxyphenyl]ethene (2) (200 mg, 0.6 mmol) was dissolved in anhydrous CH₂Cl₂ (5 mL) in a flame-dried round-bottom flask under argon. The reaction mixture was cooled at –30 °C and BBr₃ (0.70 mL of a 99% solution, 7.5 mmol) was added. The reaction was stirred at –30 °C for 10 min and at 0 °C for 50 min and TLC of the reaction mixture (hexane/EtOAc 2:1) indicated formation of a major compound and complete consumption of starting material (R_f 0.40). The crude mixture was cooled down to 0 °C, water (30 mL) was added dropwise and the solution was let to stir at rt for 10 min. Then, NaOH 5 N was added until pH 14 and the crude mixture was washed with CH₂Cl₂ (3 × 20 mL). HCl 5 N was added until pH 1 and the aqueous phase was extracted with EtOAc (3 × 30 mL). The combined organic phases were dried (Na₂SO₄), filtered and concentrated *in vacuo* to afford 3,4,5,2',4'-pentahydroxystyrene (3) (188 mg, 98% yield) as a white solid. R_f = 0.25 (hexane/EtOAc 1:1). IR (film) ν cm⁻¹: 2933 (Ar–H), 2836 (=C–H), 1205 (Ar–O), 1128 (C–O). NMR ¹H (CDCl₃, 300 MHz) δ (ppm): 6.40–6.70 (m, 2H, H-5', H-3'). 6.73 (s, 2H, H-2, H-6), 7.62 (d, *J* = 12 Hz, 1H, Ar–CH=CH–Ar), 7.78 (d, *J* = 12 Hz, 1H, Ar–CH=CH–Ar), 8.37 (s, 1H, H-6'). NMR ¹³C (CDCl₃, 75.5 MHz) δ (ppm): 101.7 (CH, C-3'), 106.4 (CH, C-5'), 118.2 (CH, Ar–CH=CH–Ar), 123.4 (CH, Ar–CH=CH–Ar), 125.6 (CH, C-2, C-6), 126.8 (CH, C-6'), 128.7 (C–OH), 134.0 (C-1), 137.7 (C–OH), 139.3 (C-1'), 146.5 (2 x C–OH), 152.1 (C–OH). HRMS-ESI (-) *m/z*: Calculated for C₁₄H₁₂O₅ (M – H): 259.0685. Found: 259.0663.

(*E*)-1,3-Dimethoxy-5-(4-methoxystyryl)benzene (4). To a solution of resveratrol (0.2 g, 0.876 mmol, 1 eq) in DMF (4 mL), anhydrous potassium carbonate (0.727 g, 5.258 mmol, 6 eq) and 1 mL (16.063 mmol, excess) of methyl iodide were added. The mixture was left to react at room temperature and after 6 h, an additional 0.5 mL (8.032 mmol) of alkylating agent was added. The next day an additional 0.5 mL of methyl iodide was added. The reaction was stopped after three days since it was observed by thin layer that there was no starting product left and a new product with R_f 0.743 (hexane/EtOAc (5:5)) has been detected. Then water (15 mL) was added to the reaction crude and extracted with diethyl ether (3 × 20 mL). The combined organic phases were washed with an aqueous solution of NaOH (2 N) (3 × 20 mL) to eliminate the starting product and the possible by-products formed

derived from the mono or dialkylation. The organic phase was dried over anhydrous sodium sulfate, which was subsequently filtered and the solvent was evaporated to dryness on a rotary evaporator, obtaining 4 as a white solid (237 mg, 100% yield). R_f = 0.7463 (hexane/EtOAc (5:5)). mp: 58–59 °C (Bibliography 57 °C [1e,21]). NMR ¹H (CDCl₃, 400 MHz) δ (ppm): 3.827 (s, 3H, C-4'-O-CH₃); 3.833 (s, 6H, C-3-O-CH₃, C-5-O-CH₃); 6.40 (t, *J* = 2.3 Hz, 1H, H-4); 6.68 (d, *J* = 2.3 Hz, 2H, H-2, H-6); 6.91 (d, *J* = 8.6 Hz, 2H, H-3', H-5'); 6.92 (d, *J* = 16.3 Hz, 1H, –HC=C); 7.06 (d, *J* = 16.3 Hz, 1H, –HC=C); 7.46 (d, *J* = 8.6 Hz, 2H, H-2', H-6'). NMR ¹³C (CDCl₃, 100.6 MHz) δ (ppm): 55.27 (CH₃, C-4-OCH₃); 55.31 (CH₃ (x 2), C-3-OCH₃, C-5-OCH₃); 99.9 (CH, C-4); 104.6 (CH, C-2, C-6); 114.5 (CH, C-3', C-5'); 127.0 (CH, CH=C); 128.2 (CH, C-2', C-6'); 129.1 (CH, CH=C); 130.3 (C-1'); 140.2 (C-1); 160.0 (C-4'); 161.6 ((x 2), C-3, C-5). HMRS-ESI (+) *m/z*: Calculated for C₁₇H₁₈O₃: 271.1334 [M+H]⁺. Found: 271.1323 [M+H]⁺.

(*E*)-2,2'-(5-(4-(2-Hydroxyethoxy)styryl)-1,3-phenylene)bis(oxy)bis(ethan-1-ol) (5). Resveratrol (1 g, 4.381 mmol, 1 eq) was introduced into a 100 mL capacity flask equipped with magnetic stirring and previously flamed under an argon atmosphere and dissolved in 30 mL acetone, then anhydrous potassium carbonate (3.6 g, 26.043 mmol, 12 eq) was added to the solution. The mixture was cooled with an external ice bath, then bromoethanol (3 mL, d = 1.763 g/mL, 42.274 mmol, excess) was added. The mixture was left to react at room temperature for 30 days, adding 0.3 mL (4.227 mmol) of alkylating agent every 3 days. Thin layer chromatography shows that after three days of reaction there was still mostly starting product and that monoalkylation product was formed. More alkylating agent (0.3 mL, d = 1.763 g/mL, 4.227 mmol) was added on reaction days 3, 5 and 14. On day 14 of the reaction, another six equivalents of potassium carbonate and 50 mL of ethanol were also added to improve the solubility of the mono- and dialkylated products and thus favor their reactivity. The solvent was evaporated to dryness on a rotary evaporator under vacuum and the residue obtained was dissolved in ethyl acetate and washed three times with an acidic aqueous solution (1 N HCl). The organic phase was dried over anhydrous sodium sulfate, which was subsequently filtered and the solvent was evaporated to dryness on a rotary evaporator. The residue obtained was purified by silica gel column chromatography using mixtures of hexane/ethyl acetate and ethyl acetate/methanol of increasing polarity as eluents. The compound 5 eluted with a polarity of 100% ethyl acetate and a white gummy solid is obtained (110 mg, 7% yield). R_f: 0,095 (hexane/ethyl acetate (3:7)). mp: 100–102 °C (hexane/ethyl acetate). NMR ¹H (CDCl₃, 400 MHz) δ (ppm): 3,96 (bs, 6H, O–CH₂–CH₂–OH (X3)); 3,96 (s, 3H, O–CH₂–CH₂–OH); 4,09 (t, *J* = 4,8 Hz, 6H, O–CH₂–CH₂–OH (X3)); 6,42 (t, *J* = 2,2 Hz, 1H, H-4); 6,75 (d, *J* = 2,2 Hz, 2H, H-2, H-6); 6,95 (d, *J* = 8,8 Hz, 2H, H-3', H-5'); 7,01 (d, *J* = 16,4 Hz, 1H, –HC=C); 7,20 (d, *J* = 16,4 Hz, 1H, –HC=C); 7,52 (d, *J* = 8,8 Hz, 2H, H-2', H-6'). NMR ¹³C (CDCl₃, 100.6 MHz) δ (ppm): 61,6 (CH₂, O–CH₂–CH₂–OH); 70,9 (CH₂, O–CH₂–CH₂–OH); 101,9 (CH, C-4); 106,3 (CH, C-2, C-6); 116,1 (CH, C-3', C-5'); 127,9 (CH, CH=C); 129,3 (CH, C-2', C-6'); 130,1 (CH, CH=C); 131,6 (C-1'); 141,4 (C-1); 160,7 (C-4'); 162,3 ((x 2), C-3, C-5). EM, ESI (+) *m/z*: Calculated for C₂₀H₂₄O₆ = 317.1389 [M+H]⁺. Found: 361.1656 [M+H]⁺, 383.1430 [M+Na]⁺.

(*E*)-5-(4-(Pivaloyloxy)styryl)-1,3-phenylenebis(2,2-dimethylpropanoate) (6). Resveratrol (1) (0.1 g, 0.438 mmol, 1 eq) suspended in 15 mL of dichloromethane was introduced into a 100 mL flask equipped with magnetic stirring. Anhydrous potassium carbonate (0.302 g, 2.190 mmol, 5 eq) was then added and cooled with an external water and ice bath. Pivaloyl chloride (0.324 mL, d = 0.979 g/mL, 5.256 mmol, 12 eq) was also added and the mixture allowed to react at room temperature for 16 h. After this time a reaction control was performed by thin layer chromatography and the starting product was observed but not the final product. The reaction crude showed a white precipitate corresponding to the unreacted starting material. In order to improve the solubility of resveratrol, anhydrous acetone (15 mL) and excess of triethylamine (5 mL, d = 0.726 g/mL, 35.87 mmol) were added and allowed to react for 24 h. The solvent was evaporated to dryness on a rotary evaporator with

the aid of vacuum and the remaining residue was extracted with diethyl ether (3 × 15 mL) and distilled water (15 mL). The organic phases were combined and washed with 2 N NaOH (2 × 15 mL) and then dried over anhydrous Na₂SO₄, which was filtered and the solvent was evaporated to dryness. The crude reaction was purified by column chromatography on silica gel in CombiFlash® Rf using mixtures of hexane and ethyl acetate of increasing polarity as eluents. The final product, a white solid, eluted with a polarity of hexane/EtOAc (86:14). (0.289 mmol, 138 mg, 66% yield). R_f: 0.55 (hexane/EtOAc (9: 1)). mp: 141–144 °C (Hexane/EtOAc). IR (KBr) ν cm⁻¹: 2963 (CH); 1757 (C=O); 1508 (C=C); 1166 (Ar-O); 1103 (C-O). NMR ¹H (CDCl₃, 400 MHz) δ (ppm): 1.371–1.374 (bs, 27H, CH₃ (x 9)); 6.78 (t, *J* = 2.0 Hz, 1H, H-4); 6.98 (d, *J* = 16.4 Hz, 1H, -HC=C); 7.07 (d, *J* = 8.6 Hz, 2H, H-3', H-5'); 7.09 (d, *J* = 16.4 Hz, 1H, HCC); 7.09 (d, *J* = 2.1 Hz, 2H, H-2, H-6); 7.49 (d, *J* = 8.6 Hz, 2H, H-2', H-6'). NMR ¹³C (CDCl₃, 100.6 MHz) δ (ppm): 26.9 (CH₃ (x 9)); 39.0 (Cq, C-CH₃ (x 3)); 114.6 (CH, C-4); 117.0 (CH, C-2, C-6); 122.2 (CH, C-3', C-5'); 127.5 (CH, CH=C); 127.9 (CH, C-2', C-6'); 123.0 (CH, CH=C); 134.7 (C-1'); 139.9 (C-1); 151.4 (C-4'); 152.3 (C-3, C-5); 177.3 (C=O (x 2)); 17.7 (CO). HMRS-ESI (+) *m/z*: Calculated for C₂₉H₃₆O₆ = 481.2590 [M+H]⁺. Found: 481.2601 [M+H]⁺, 503.2426 [M+Na]⁺, 498.2869 [M + NH₄]⁺ 978.5389, [2 M + NH₄]⁺, 983.4948 [2 M + Na]⁺.

(E)-5-(4-(Dodecanoyloxy)styryl)-1,3-phenylene didodecanoate (7). Resveratrol (0.1 g, 0.438 mmol, 1 eq) dissolved in 15 mL of acetone was introduced into a 50 mL flask equipped with magnetic stirring and previously flamed under argon atmosphere. Triethylamine (0.3 mL, *d* = 0.726 g/mL, 2.190 mmol, 5 eq) was added and allowed to react at room temperature for 10 min. It was then cooled with an external water and ice bath and dodecanoyl chloride (0.625 mL, *d* = 0.92 g/mL, 2.628 mmol, 6 eq) was added. The mixture was allowed to react at room temperature for four days. The white precipitate formed was filtered by gravity and the solvent was evaporated to dryness until a yellow oil is obtained. The NMR-¹H spectrum showed that the residue contains the final product but also dodecanoyl chloride. In order to remove it, it was washed with water and 2 N NaOH, but the product was not completely purified. Acid chloride could not be removed by hydrolysis as the ester of the final product was also unstable under these conditions.

The ester **7** was purified by silica gel column chromatography, the product was eluted with a polarity of hexane/ethyl acetate (98: 2) and was obtained in the form of white rubber (176 mg, 52% yield). R_f: 0.83 (hexane/EtOAc (9: 1)). mp: 43–45 °C (hexane/EtOAc). NMR ¹H (CDCl₃, 400 MHz) δ (ppm): 0.88 (t, *J* = 6.7 Hz, 9H, CH₃ (x 3)); 1.25–1.29 (m, 48H, CH₂ (x 24)); 1.71–1.79 (m, 6H, CO-CH₂-CH₂-); 2.55 (t, *J* = 7.6 Hz, 6H, CO-CH₂-CH₂-); 6.80 (t, *J* = 2.0 Hz, 1H, H-4); 6.97 (d, *J* = 16.3 Hz, 1H, -HC=C); 7.06 (d, *J* = 16.3 Hz, 1H, -HC=C); 7.08 (d, *J* = 8.6 Hz, 2H, H-3', H-5'); 7.10 (d, *J* = 2.1 Hz, 2H, H-2, H-6); 7.48 (d, *J* = 8.7 Hz, 2H, H-2', H-6'). NMR ¹³C (CDCl₃, 100.6 MHz) δ (ppm): 14.2 (CH₃ (x 9)); 22.8 (CH₂ (x 3), -CH₂-CH₂-CH₃); 25.0 (CH₂ (x 3), -CO-CH₂-CH₂); 29.3 (CH₂); 29.4 (CH₂); 29.5 (CH₂); 29.6 (CH₂); 29.8 (CH₂ (x 2)); 32.1 (CH₂ (x 3), -CH₂-CH₂-CH₃); 34.6 (CH₂ (x 3), -CO-CH₂-CH₂); 112.6 (CH, C-3', C-5'); 115.1 (CH, C-4); 117.5 (CH, C-2, C-6); 127.9 (CH, CH=C); 128.3 (CH, C-2', C-6'); 130.3 (CH, CH=C); 135.1 (C, C-1'); 140.3 (C-1); 151.4 (C-4'); 152.3 (C-3, C-5); 172.8 (C=O (x 2)); 173.2 (C=O). HMRS-ESI (+) *m/z*: Calculated for C₅₀H₇₈O₆ = 797.5696 [M+Na]⁺. Found: 797.5731 [M+Na]⁺, 792.6151 [M + NH₄]⁺, 1568.1999 [2 M + NH₄]⁺, 1573.1593 [2 M + Na]⁺.

6-Hydroxy-2-(3,4,5-trimethoxyphenyl)isobenzofuran (8). 7-Hydroxy-3-(3,4,5-trimethoxyphenyl)chromen-2-one (150 mg, 0.46 mmol) was dissolved in ethanol (30 mL) and HCl 2 N (120 mL) was added. The reaction was refluxed under stirring for 16 h and TLC of the crude mixture (hexane/EtOAc 2:1) indicated formation of a new compound (R_f 0.35) and complete consumption of starting material (R_f 0.20). The ethanol was evaporated *in vacuo* and the aqueous phase was extracted with CH₂Cl₂ (3 × 30 mL). The combined organic phases were dried (Na₂SO₄), filtered and concentrated *in vacuo*. The crude residue was purified by silica gel flash column chromatography (hexane/EtOAc 2:1) to afford the desired compound **8** (25 mg, 18% yield) as a white solid.

The reaction was scaled up using 660 mg of 7-hydroxy-3-(3,4,5-trimethoxyphenyl)chromen-2-one to obtain **8** (174 mg, 29% yield) as a white solid. R_f = 0.35 (hexane/EtOAc 2:1). mp: 230–232 °C (hexane/EtOAc). IR (film) ν cm⁻¹: 3208 (Ar-OH), 1607, 1510, 1446, 1415 (=C-H), 1218 (Ar-O), 1121 (C-O). NMR ¹H (CDCl₃, 200 MHz) δ (ppm): 3.89 (s, 3H, O-CH₃), 3.92 (s, 6H, O-CH₃ (x 2)), 6.85 (dd, *J* = 2 Hz, *J* = 8 Hz, 1H, H-5), 6.91 (s, 2H, H-2', H-6'), 6.93 (d, *J* = 2 Hz, 1H, H-7), 7.42 (d, *J* = 8.0 Hz, 1H, H-4), 7.77 (s, 1H, H-3). NMR ¹³C (CDCl₃, 50 MHz) δ (ppm): 56.4 (CH₃, OCH₃ (x 2)), 61.2 (CH₃, OCH₃), 103.1 (CH, C-3), 106.4 (CH, C-2', C-6'), 114.1 (C, C-4a), 129.4 (CH, C-7), 130.9 (CH, C-5), 138.8 (C, C-1'), 140.8 (CH, C-4), 153.4 (C-3', C-4', C-5'), 155.3 (C-6), 160.7 (C-2), 161.9 (C-7a). MS (ESI (+)) *m/z* (%): 300 (M⁺, 3.12), 285 (M⁺ - 15, 21), 255 (M⁺ - 45, 11.73), 181 (M⁺-C₁₀H₁₃O₃, 27.61).

2-(3,4,5-Trihydroxyphenyl)-6-hydroxybenzofuran (9). 6-Hydroxy-2-(3,4,5-trimethoxyphenyl)isobenzofuran **9** (60 mg, 0.2 mmol) was dissolved in anhydrous CH₂Cl₂ (30 mL) in a flame-dried round-bottom flask under argon. The reaction was cooled at -30 °C and BBr₃ (0.4 mL of a 99% solution, 4.2 mmol) was added. The resulting mixture was stirred for 10 min at -30 °C and allowed to warm at rt for 3 h. Then, TLC of the reaction mixture (hexane/EtOAc 2:1) indicated formation of a new compound (R_f 0.10) and complete consumption of starting material (R_f 0.35). The crude mixture was cooled down to 0 °C and water (30 mL) was added dropwise. The solution was let to stir at rt for 10 min. Then, NaOH 5 N was added until pH 10 and washed with CH₂Cl₂ (3 × 20 mL). Finally, HCl 5 N was added until pH 1 and the aqueous phase was extracted with EtOAc (3 × 30 mL). The combined organic phases were dried (Na₂SO₄), filtered and concentrated *in vacuo* to afford the desired compound **9** (32 mg, 62% yield) as a yellow solid. R_f = 0.10 (hexane/EtOAc 2:1). mp: 292–295 °C (hexane/EtOAc). IR (film) ν cm⁻¹: 3389, 3339, 3197 (Ar-OH), 2922 (Ar-H), 2852 (Ar-H), 1237 (Ar-O). NMR ¹H (Acetone-d₆, 200 MHz) δ (ppm): 6.72 (dd, *J* = 2 Hz, *J* = 8 Hz, 1H, H-5), 6.73 (s, 2H, H-2', H-6'), 6.74 (d, *J* = 2 Hz, 1H, H-7), 7.43 (d, *J* = 8.0 Hz, 1H, H-4), 7.77 (s, 1H, H-3). NMR ¹³C (Acetone-d₆, 100 MHz) δ (ppm): 102.8 (CH, C-3), 108.7 (CH, C-2', C-6'), 113.9 (CH, C-7), 124.4 (C, C-3a), 130.39 (CH, C-5), 134.3 (C-1'), 139.7 (CH, C-4), 146.3 (C-3', C-4', C-5'), 156.0 (C-6), 160.9 (C-2), 161.5 (C-7a). HRMS-ESI (-) *m/z* (%): Calculated for C₁₄H₁₀O₅-H (M - H): 257.0528. Found: 257.0468.

2-(3,5-Dimethoxyphenyl)benzofuran-6-ol (10). Compound **22** (0.113 g, 0.38 mmol, 1.0 eq) was dissolved in ethanol in a 100 mL flask and 90 mL of 2 N HCl were added. The mixture was allowed to react under constant stirring at 120 °C for 16 h. The solvent was evaporated on a rotary evaporator, ice was added to the crude residue and extracted with dichloromethane (3 × 20 mL). The organic phase was dried over anhydrous sodium sulfate, which was then filtered and the solvent is evaporated to dryness. The benzofuran **10** obtained was a purple solid (102.2 mg, 100% yield). R_f: 0.4 (hexane/ethyl acetate (5: 5)). Melting point: 163–164 °C (ethyl acetate). NMR ¹H ((CD₃)₂CO, 400 MHz) δ (ppm): 3.82 (s, 6H, CH₃-O (x 2)); 6.51 (t, *J* = 2 Hz, 1H, H-4'); 6.80 (d, *J* = 2 Hz, 1H, H-7); 6.88 (dd, *J*₁ = 2 Hz, *J*₂ = 8 Hz, 1H, H-5); 6.93 (d, *J* = 2 Hz, 2H, H-2', H-6'); 7.57 (d, *J* = 8 Hz, 1H, H-4); 8.07 (s, 1H, H-3); 9.77 (bs, 1H, OH). NMR ¹³C ((CD₃)₂CO, 100.6 MHz) δ (ppm): 55.8 (CH₃-O (x 2)); 101.2 (CH, C-4'); 103.2 (CH, C-7); 107.9 (CH, C-2', C-6'); 114.4 (CH, C-5); 124.7 (C-1'); 131.3 (CH, C-4); 138.8 (C-3a); 142.1 (CH, C-3); 157.0 (C-6); 161.4 (C-7a); 162.2 (C-3' and C-5'); 162.6 (C-2). HMRS-ESI (+) *m/z*: Calculated for C₁₆H₁₄O₄ = 271.0970 [M + H]⁺. Found: 271.0618 [M + H]⁺.

5-(6-Hydroxybenzofuran-2-yl)benzene-1,3-diol (11). Compound **10** (0.081 g, 0.230 mmol, 1 eq) was dissolved in 5 mL of anhydrous dichloromethane in a 50 mL capacity flask previously flamed with argon and cooled externally to -20 °C. BBr₃ (0.144 mL, 1.50 mmol, *d* = 2.60 g/mL, 5.0 eq) was then added and the resulting mixture was stirred at room temperature, stirring constantly for 16 h 15 mL of distilled water was added to the crude residue and extracted with ethyl acetate (3 × 20 mL). The organic phase was dried over anhydrous sodium sulfate, which was then filtered and the solvent was evaporated to dryness. The residue obtained was purified by chromatography on silica gel. The expected

benzofuran **11** elutes with a polarity of hexane/EtOAc (54:46). (31,5 mg, 41% yield). R_f : 0.125 (hexane/EtOAc (5: 5)). mp: 43–45 °C (hexane/EtOAc). NMR ^1H ((CD₃)₂CO, 400 MHz) δ (ppm): 6.51 (t, J = 2 Hz, 1H, H-4'); 6.73 (d, J = 2 Hz, 2H, H-2', H-6'); 6.76 (d, J = 2 Hz, 1H, H-7); 6.83 (dd, J_1 = 2 Hz, J_2 = 8.5 Hz, 1H, H-5); 7.56 (d, J = 8.5 Hz, 1H, H-4); 7.94 (s, 1H, H-3). NMR ^{13}C ((CD₃)₂CO, 100.6 MHz) δ (ppm): 102.7 (CH, C-7); 103.3 (CH, C-4'); 107.8 (CH, C-2', C-6'); 114.1 (CH, C-3); 124.2 (C-4a); 136.7 (CH, C-5); 138.2 (C-1'); 141.0 (C-4); 156.3 (C-6); 159.1 (C-3' and C-5'); 160.8 (C-7a); 162.3 (C-2). Anal. Calcd. for C₁₄H₁₀O₄: C, 69.42; H, 4.16. Found: C, 69.56; H, 4.11.

6-(Benzyl)-2-(2,5-dimethoxyphenyl)indole (12). 3-Benzoxaniline (2.3 g, 6.95 mmol) was dissolved in *N,N*-dimethylaniline (25 mL) in a flame-dried round-bottom flask under argon. The mixture was heated to 150 °C, 2'-bromo-2,5-dimethoxyacetophenone (**113**) (1 g, 2.32 mmol) was added and the mixture was heated at 165 °C for 1 h. Then, TLC of the crude mixture (hexane/EtOAc 8:2) indicated formation of a new compound (R_f 0.45) and complete consumption of starting materials (R_f 0.25, R_f 0.10). The crude mixture was dissolved in EtOAc (50 mL), washed with 2 N HCl (4 × 50 mL) and the aqueous phase were extracted with EtOAc (3 × 30 mL). The combined organic phases were dried (Na₂SO₄), filtered and concentrated *in vacuo*. The crude residue was purified by aluminum oxide flash column chromatography (hexane/EtOAc 8:2). The residue was recrystallized (hexane/EtOAc 8:2) to afford 6-(benzyl)-2-(2,5-dimethoxyphenyl)indole (**12**) (740 mg, 53% yield) as a white solid. The product is unstable and must be put in the fridge and protected from the light. R_f = 0.45 (hexane/EtOAc 8:2). mp: 114–117 °C (hexane/EtOAc). IR (film) ν cm⁻¹: 3436 (NH), 2923 (C-H), 1624, 1484, 1461 (Ar-H, C=C-H), 1213, 1182 (Ar-O), 1040, 1023 (C-O). NMR ^1H (CDCl₃, 400 MHz) δ (ppm): 3.81 (s, 3H, CH₃-O), 3.91 (s, 3H, CH₃-O), 5.10 (s, 2H, CH₂-O), 6.75 (dd, J = 3.2 Hz, J = 9.2 Hz, 1H, H-4'), 6.81 (d, J = 2 Hz, 0.8 Hz, 1H, H-6'), 6.86 (dd, J = 2 Hz J = 8.4 Hz, 1H, H-5), 6.91 (d, J = 8.4 Hz, 1H, H-4), 6.94 (d, J = 2.4 Hz, 1H, H-7), 7.34–7.37 (m, 2H, H-3, H-3'), 7.39–7.44 (t, J = 6.8 Hz, 2H, H-3', H-5''), 7.48–7.55 (m, 3H, H-2'', H-4'', H-6''). NMR ^{13}C (CDCl₃, 100 MHz) δ (ppm): 56.2 (CH₃, OCH₃), 56.8 (CH₃, OCH₃), 70.9 (CH₂, CH₂-OBn), 96.0 (CH, C-7), 100.3 (CH, C-3), 111.3 (CH, C-6'), 113.3 (CH, C-5), 113.5 (CH, C-3'), 113.6 (CH, C-4'), 121.3 (CH, C-4), 121.9 (C, C-3a), 123.0 (C-1'), 127.8 (CH, C-2'', C-6''), 128.1 (CH, C-3'', C-5''), 128.9 (CH, C-4''), 135.2 (C-7a), 137.2 (C-1''), 137.9 (C-2''), 150.4 (C-6), 154.5 (C-2'), 155.9 (C, C-5'').*Interchangeable. MS-EI m/z (%): 359 (M⁺, 24), 268 (100). Anal. Calcd. for C₂₃H₂₁NO₂: C, 80.44; H, 5.15. Found: C, 80.56; H, 5.45.

6-Hydroxy-2-(2,5-dimethoxyphenyl)indole (13). 6-(Benzyl)-2-(2,5-dimethoxyphenyl)indole (80 mg, 0.22 mmol) was dissolved in methanol (30 mL) and ethyl acetate (5 mL). 10% palladium on charcoal catalyst (8 mg, 10% w/w) in EtOAc (5 mL) was added and the reaction mixture was put under hydrogen atmosphere under stirring for 2 days. Then, TLC of the crude mixture (hexane/EtOAc 8:2) indicated formation of a new compound (R_f 0.10) and complete consumption of starting material (R_f 0.45). The crude mixture was filtered and concentrated *in vacuo* to afford 81 mg of a white solid. The residue was purified by aluminum oxide flash column chromatography (hexane/EtOAc 6:4) to afford the desired compound **13** (33 mg, 55% yield) as a white solid. The product was unstable, must be put in the fridge, and protected from the light. R_f = 0.10 (hexane/EtOAc 8:2). mp: 50–52 °C (hexane/EtOAc). IR (film) ν cm⁻¹: 3433 (Ar-OH, NH), 2922 (C-H), 1624, 1498, 1450 (Ar-H, C=C-H), 1211, 1164 (Ar-O), 1041, 1020 (C-O). NMR ^1H (Acetone-d₆, 300 MHz) δ (ppm): 3.83 (s, 3H, OCH₃), 3.94 (s, 3H, OCH₃), 5.19 (bs, 1H, OH), 6.69 (dd, J = 2.2 Hz, J = 8.4 Hz, 1H, H-5), 6.79 (s, 1H, H-3), 6.80 (dd, J = 3 Hz, J = 9 Hz, 1H, H-6'), 6.85 (d, J = 2.2 Hz, 1H, H-7), 6.92 (d, J = 9 Hz, 1H, H-4) 7.31 (d, J = 3 Hz, 1H, H-4'), 7.45 (d, J = 9 Hz 1H, H-3'). NMR ^{13}C (Acetone-d₆, 75.5 MHz) δ (ppm): 55.6 (CH₃, CH₃-O), 56.1 (CH, C-6'), CH₃, CH₃-O), 96.9 (CH, C-7), 101.5 (CH, C-3), 110.5 (CH, C-6'), 113.2 (CH, C-5), 113.6 (CH, C-3'), 113.7 (CH, C-4'), 120.9 (CH, C-4), 122.5 (C-3a), 122.8 (C-1'), 134.2 (C-7a), 138.4 (C-2), 150.7 (C-6), 154.1 (C-2'), 154.5 (C-5'). MS-EI m/z (%): 269 (M⁺, 100), 254 (M +

CH₃, 77), 239 (M + - C₂H₆, 45). Anal. Calcd. for C₁₆H₁₅NO₃: C, 71.36; H, 5.61. Found: C, 71.01; H, 5.31.

5,7-Dimethoxy-2-(4-methoxyphenyl)-1H-indole (14). The starting aniline (0.802 g, 5.2 mmol, 3 eq) dissolved in 20 mL of DMA and 2-bromo-1-(4-methoxyphenyl) ethanone (0.4 g, 1.7 mmol, 1 eq) were introduced into a 100 mL flask preheated to 150 °C. The mixture was kept under constant stirring and heated at 165 °C for 1 h. After this time the reaction was stopped. In a second attempt the reaction was maintained for 2 h, but the performance did not improve. 50 mL of HCl (2 N) was added to the reaction crude and extracted with ethyl acetate (3 × 20 mL). The organic phases were combined and dried over anhydrous Na₂SO₄, which was filtered off and the solvent was evaporated to dryness.

The crude reaction was purified by silica gel column chromatography. The final product was eluted with a polarity of hexane/ethyl acetate (86:14) and a red rubber-like product **14** was obtained. (24.7 mg, 5% yield). R_f = 0.194 (hexane/ethyl acetate (8: 2)). NMR ^1H (CDCl₃, 400 MHz) δ (ppm): 3.81 (s, 3H, CH₃-OAr); 3.87 (s, 3H, CH₃-OAr); 3.89 (s, 3H, CH₃-OAr); 6.51 (s, 1H, H-3); 6.65 (d, J = 9 Hz, 1H, H-6); 6.93–6.98 (m, 3H, H-4, H-3', H-5'); 7.84 (d, J = 9 Hz, 2H, H-2', H-6'); 8.26 (bs, 1H, NH). NMR ^{13}C (CDCl₃, 100.6 MHz) δ (ppm): 55.5 (CH₃, Ar-OCH₃); 55.6 (CH₃, Ar-OCH₃); 55.9 (CH₃, Ar-OCH₃); 98.9 (CH, C-6); 104.1 (CH, C-3); 111.2 (CH, C-4); 114.2 (CH, C-3', C-5'); 121.4 (C-7a); 127.2 (C-3a); 128.1 (C-2); 129.28 (CH, C-2', C-6'); 150.0 (C-7); 156.9 (C-5); 162.9 (C-4'). HMRS-ESI (-) m/z : Calculated for C₁₇H₁₆NO₃ = 282.1136 [M - H]⁻. Found: 282.1159 [M - H]⁻. Anal. Calcd. for C₁₇H₁₇NO₃: C, 72.07; H, 6.05. Found: C, 72.22; H, 5.89.

2-(4-Methoxyphenyl)-5,7-dimethyl-1H-indole (15). The starting aniline (0.403 g, 3.3 mmol, 3 eq) and the bromoacetophenone (0.25 g, 1.1 mmol, 1 eq) dissolved in 10 mL of DMA were added in a 100 mL flask preheated to 150 °C. The resulting mixture was heated to 165 °C for 1 h. After this time the reaction was stopped. In a second attempt the reaction was maintained for 2 h, but the yield decreased from 21% to 14%. 50 mL of HCl (2 N) was added to the reaction crude and extracted with ethyl acetate (3 × 20 mL). The organic phases were combined and dried over anhydrous Na₂SO₄, which was filtered off and the solvent was evaporated to dryness. The crude reaction was purified by silica gel column chromatography. The desired compound **15** was eluted with a polarity of hexane/ethyl acetate 9:8:0.2. (57 mg, 21% yield). R_f = 0.763 (hexane/ethyl acetate (8:2)). mp: 88–90 °C. NMR ^1H (CDCl₃, 400 MHz) δ (ppm): 2.39 (s, 3H, CH₃-Ar); 2.50 (s, 3H, CH₃-Ar); 3.87 (s, 3H, OCH₃); 6.23 (s, 1H, H-3); 6.73 (d, J = 7.9 Hz, 1H, H-6); 6.99 (d, J = 9.1 Hz, 2H, H-3', H-5'); 7.04 (d, J = 7.9 Hz, 1H, H-4); 7.13 (s, 1H, NH); 8.50 (d, J = 9.1 Hz, 2H, H-2', H-6'). NMR ^{13}C (CDCl₃, 100.6 MHz) δ (ppm): 15.7 (CH₃, Ar-CH₃); 17.7 (CH₃, Ar-CH₃); 55.4 (CH₃, Ar-OCH₃); 114.2 (CH, C-3', C-5'); 117.0 (CH, C-3); 122.4 (C-7); 124.1 (CH, C-4); 126.1 (C-3a); 126.6 (C-5); 127.5 (CH, C-6); 130.6 (C-1'); 132.1 (CH, C-2', C-6'); 135.1 (C-7a); 136.4 (C-2); 162.3 (C-4'). Anal. Calcd. for C₁₇H₁₇NO: C, 81.24; H, 6.28. Found: C, 81.61; H, 6.18.

7-Hydroxy-3-(3,4,5-trimethoxyphenyl)-chromen-2-one (21). 2,4-Dihydroxy benzaldehyde (305 mg, 2.21 mmol), 2-(3,4,5-trimethoxyphenyl)-acetic acid (500 mg, 2.21 mmol) and Et₃N (1.7 mL, 12.1 mmol) were dissolved in acetic anhydride (3 mL, 32 mmol) in a flame-dried round-bottom flask under argon. The reaction was refluxed under stirring for 3 h and TLC of the crude mixture (hexane/EtOAc 1:1) indicated formation of a green fluorescent compound (R_f 0.65) and complete consumption of starting material (R_f 0.80). CH₂Cl₂ (20 mL) was added and the crude mixture was quenched with water (30 mL). The aqueous phase was extracted with CH₂Cl₂ (3 × 30 mL) and the combined organic phases were dried (Na₂SO₄) and concentrated *in vacuo*. The crude of reaction was microdistilled at 150 °C and purified by silica gel flash column chromatography (hexane/EtOAc 8:2) to afford 7-hydroxy-3-(3,4,5-trimethoxyphenyl)-chromen-2-one (360 mg, 47% yield) as a white solid. R_f = 0.80 (hexane/EtOAc 8:2). mp: 141–143 °C (hexane/EtOAc). IR (film) ν cm⁻¹: 3210 (Ar-OH), 2919 (CH), 2848 (=C-H), 1719 (C=O), 1225 (Ar-O), 1103 (C-O). NMR ^1H (CDCl₃, 300 MHz) δ (ppm):

3.86 (s, 3H, O-CH₃), 3.89 (s, 6H, O-CH₃ (x 2)), 6.93 (s, 2H, H-2', H-5'), 7.06 (dd, *J* = 2 Hz, *J* = 8 Hz, 1H, H-6), 7.14 (d, *J* = 2 Hz, 1H, H-8), 7.54 (d, *J* = 8.0 Hz, 1H, H-5), 7.78 (s, 1H, H-4). NMR ¹³C (CDCl₃, 75.5 MHz) δ (ppm): 57.3 (CH₃, OCH₃ (x 2)), 61.5 (CH₃, OCH₃), 103.8 (CH, C-2', C-6'), 107.5 (CH, C-8), 110.0 (CH, C-6), 126.1 (C, C-4a), 129.3 (CH, C-5), 130.94 (C, C-3), 139.1 (CH, C-4), 152.4 (C-4'), 153.0 (C-3', C-5'), 154.6 (C-7), 160.1 (C-8a), 169.3 (C-2). MS EI *m/z* (%): 327 (M⁺, 92).

3-(3,5-Dimetoxifenil)-7-hidroxi-2H-croma-2-ona (22). Aldehyde **18** (0.200 g, 1.45 mmol, 1.0 eq) and acid **20** (0.284 g, 1.45 mmol, 1.0 eq) were dissolved in 2 mL of acetic anhydride and added to a 100 mL flask. Then triethylamine (1.12 mL, *d* = 0.726 g/mL, 0.813 g, 7.94 mmol, *d* = 0.726 g/mL, 5.55 eq) was added and the resulting mixture was heated to reflux (150 °C) for 16 h. Ice was added to the reaction crude and extracted with dichloromethane (3 × 20 mL). The organic phase was dried over anhydrous sodium sulfate, which was then filtered and the solvent was evaporated to dryness. The residue obtained was purified by silica gel column chromatography and the expected product was eluted with a polarity of hexane/ethyl acetate (60:40) and a brown solid was obtained (431 mg, 100% yield). *R*_f: 0.49 (hexane/ethyl acetate (5: 5)). mp: 150–152 °C (hexane/ethyl acetate). NMR ¹H (CDCl₃, 400 MHz) δ(ppm): 3.83 (s, 6H, CH₃-O (x 2)); 6.52 (t, *J* = 2 Hz, 1H, H-4'); 6.83 (d, *J* = 2 Hz, 2H, H-2', H-6'); 7.07 (dd, *J*₁ = 2 Hz, *J*₂ = 8 Hz, 1H, H-6); 7.15 (d, *J* = 2 Hz, 1H, H-8); 7.53 (d, *J* = 8 Hz, 1H, H-5); 7.79 (s, 1H, H-4). NMR ¹³C (CDCl₃, 100.6 MHz) δ(ppm): 55.4 (CH₃, CH₃-O (x 2)); 101.3 (CH, C-4'); 107.0 (CH, C-2', C-6'); 110.2 (CH, C-8); 117.7 (C, C-4a); 118.8 (CH, C-6); 127.9 (C, C-3); 129.1 (CH, C-5); 136.7 (C, C-1'); 139.9 (CH, C-4); 153.5 (C, C-8a); 160.6 (C, C-7); 161.3 (C, C-3', C-5'); 169.4 (C, C=O). HMRS-ESI (+) *m/z*: Calculated for C₁₇H₁₃O₅ = 297.0763 [M - H]⁻. Found: 297.0778 [M - H]⁻.

4.2. Pharmacology

4.2.1. MTT assay and growth inhibition [26]

Cell survival was determined by colorimetric 3-(4,5-dimethylthiazol-2-yl)-2,5-diphenyltetrazolium bromide (MTT) assay which measures mitochondrial activity in viable cells. Cells (1.5 × 10⁵) were plated in each well of a 6-well plate, allowed to adhere overnight and then the culture medium was replaced with fresh media. Cells were treated with *resveratrol* or other compounds at concentrations of 10, 50 and 100 μM for 24 h. Control groups were treated with DMSO equal to the highest percentage of (<0.1%) solvent used in experimental conditions for MTT assay. After 72 h the medium was replaced with fresh medium. MTT was freshly prepared at 5 mg/mL in PBS and passed through a filter (pore size, 0.2 μM). An aliquot of 2 mL of MTT stock solution was added to each well, and the plate was incubated at 37 °C for 3 h in humidified 5% CO₂ incubator. After 3 h, media were removed and formazan crystals were dissolved in 1 mL of DMSO for 15 min with gentle agitation. The optical density of each well was measured with a spectrophotometer equipped with a 550 nm filter.

4.2.2. OIDD Lilly tests

The Lilly tests (KRas inhibition and antiangiogenesis activities) were carried out according the procedures indicated in the OIDD-Lilly program (Open Innovation Drug Discovery - Eli Lilly) (<https://openinnovati.on.lilly.com>) [27].

Declaration of competing interest

The authors declare that they have no known competing financial interests or personal relationships that could have appeared to influence the work reported in this paper.

Data availability

The data that has been used is confidential.

Acknowledgments

OIDD screening data supplied courtesy of Eli Lilly and Company—used with Lilly's permission. The SGR (2017–2021) Generalitat de Catalunya (Spain) are gratefully acknowledged for their financial support.

Appendix A. Supplementary data

Supplementary data to this article can be found online at <https://doi.org/10.1016/j.ejmech.2022.114962>.

References

- a) P. Langcake, R.J. Pryce, The production of resveratrol by vitis vinifera and other members of the vitaceae as a response to infection or injury, *Physiol. Plant Pathol.* 9 (1976) 77–86, [https://doi.org/10.1016/0048-4059\(76\)90077-1](https://doi.org/10.1016/0048-4059(76)90077-1);
 - b) M. López, F. Martínez, C. Del Valle, C. Orte, M. Miró, Analysis of phenolic constituents of biological interest in red wines by high-performance liquid chromatography, *J. Chromatogr. A* 922 (2001) 359–363, [https://doi.org/10.1016/S0021-9673\(01\)00913-X](https://doi.org/10.1016/S0021-9673(01)00913-X);
 - c) B.C. Akınwumi, K.A.M. Bordun, H.D. Anderson, Biological activities of stilbenoids, *Int. J. Mol. Sci.* 19 (2018) 792, <https://doi.org/10.3390/ijms19030792>;
 - d) N. Elmali, O. Baysal, A. Harma, I. Esenkaya, B. Mizrak, Effects of resveratrol in inflammatory arthritis, *Inflammation* 30 (2007) 1–6. <https://link.springer.com/article/10.1007/s10753-006-9012-0>;
 - e) S.H. Tsai, S.Y. Lin-Shiau, J.K. Lin, Suppression of nitric oxide synthase and the down-regulation of the activation of NFκB in macrophages by resveratrol, *Br. J. Pharmacol.* 126 (1999) 673–680, <https://doi.org/10.1038/sj.bjp.0702357>;
 - f) F. Orsini, L. Verotta, M. Lecchi, R. Restano, G. Curia, E. Redaelli, E. Wanke, Resveratrol derivatives and their role as potassium channels modulators, *J. Nat. Prod.* 67 (2004) 421–426, <https://doi.org/10.1021/np0303153>.
- a) N. Koeberle, O. Werz, Multitarget approach for natural products in inflammation, *Drug Discov. Today* 19 (2014) 1871–1882, <https://doi.org/10.1016/j.drudis.2014.08.006>.
- a) M. Larrosa, J. Tomé-Carneiro, M.J. Yáñez-Gascón, D. Alcántara, M.V. Selam, D. Beltran, M.T. García-Conesa, C. Urbán, R. Lucas, F. Tomás-Barberán, J. C. Morales, J.C. Espin, Preventive oral treatment with resveratrol pro-drugs drastically reduce colon inflammation in rodents, *J. Med. Chem.* 53 (2010) 7365–7376, <https://doi.org/10.1021/jm1007006>;
 - b) M.A.E. Reza-Ahmadi, Resveratrol-A comprehensive review of recent advances in anticancer drug design and development, *Eur. J. Med. Chem.* 200 (2020), 112356, <https://doi.org/10.1016/j.ejmech.2020.112356>.
- a) P. Peñalver, E. Belmonte-Reches, N. Adan, M. Caro, M.L. Mateos-Martín, M. Delgado, E. González-Rey, J.C. Morales, Alkylated resveratrol prodrugs and metabolites as potential therapeutics for neurodegenerative diseases, *Eur. J. Med. Chem.* 146 (2018) 123–138, <https://doi.org/10.1016/j.ejmech.2018.01.037>;
 - b) V. Cardilea, R. Chillembi, L. Lambardoa, S. Sciuotob, C. Spataforab, C. Tringalib, Antiproliferative activity of methylated analogues of E- and Z-resveratrol, *Z. Naturforsch.* 62c (2007) 189–195, <https://doi.org/10.1515/znc-2007-3-406>;
 - c) B. De Filippis, A. Ammazalorso, M. Fantacuzzi, L. Giampietro, C. Maccallini, R. Amoroso, Anticancer activity of stilbene-based derivatives, *ChemMedChem* 12 (2017) 558–5570, <https://doi.org/10.1002/cmdc.201700045>;
 - d) E. Giancchetti, A. Fierabracci, Insights on the effects of resveratrol and some of its derivatives in cancer and autoimmunity: a molecule with a dual activity, *Antioxidants* 9 (2020) 91, <https://doi.org/10.3390/antiox9020091>;
 - e) M. Ang, L. Cai, G.O. Udeani, K.V. Slowing, C.F. Thomas, C.W. Beecher, H. H. Fong, N.R. Farnsworth, A.D. Kinghorn, R.G. Mehta, Cancer chemopreventive activity of resveratrol, a natural product derived from grapes, *Science* 275 (1997) 218–220. <https://www.science.org/doi/10.1126/science.275.5297.218>;
 - f) B.B. Aggarwal, A. Bhardwaj, R.S. Aggarwal, N.P. Seeram, S. Shishodia, Y. Takada, Role of resveratrol in prevention and therapy of cancer: preclinical and clinical studies, *Anticancer Res.* 24 (2004) 2783–2840;
 - g) V.P. Androustopoulos, L. Fragiadaki, D.A. Spandidos, A. Tosca, The resveratrol analogue, 3,4,5,4'-trans-tetramethoxystilbene, inhibits the growth of A375 melanoma cells through multiple anticancer modes of action, *Int. J. Oncol.* 49 (2016) 1305–1314, <https://doi.org/10.3892/ijo.2016.3635>;
 - h) X. Zheng, L.Y. Yu, X. Yao, B. Ly, Z.H. Yang, Q.T. Zheng, H.Y. Duan, C. Song, H. L. Xie, Synthesis and anti-cancer activities of resveratrol derivatives, *Open J. Med. Chem.* 6 (2016) 51–57, <https://doi.org/10.4236/ojmc.2016.63005>;
 - i) S. Sale, R.D. Verschoyle, D. Boocock, D.J. Jones, N. Wilsher, K.C. Ruparelia, Pharmacokinetics in mice and growth-inhibitory properties of the putative cancer chemopreventive agent resveratrol and the synthetic analogue trans 3,4,5,4'-tetramethoxystilbene, *Br. J. Cancer* 90 (2004) 736–744.
- a) S. Das, H.S. Lin, P.C. Ho, K.Y. Ng, The impact of aqueous solubility and dose on the pharmacokinetic profiles of resveratrol, *Pharm. Res. (N. Y.)* 25 (2008) 2593–2600, <https://doi.org/10.1007/s11095-008-9677-1>;
 - b) F. Silva, A. Figueiras, E. Gallardo, C. Nerín, F.C. Domingues, Strategies to improve the solubility and stability of stilbene antioxidants: a comparative study between cyclodextrins and bile acids, *Food Chem.* 145 (2014) 115–125, <https://doi.org/10.1016/j.foodchem.2013.08.034>.

- [6] a) L.X. Wang, A. Heredia, H. Song, Resveratrol glucuronides as the metabolites of resveratrol in humans: characterization, synthesis, and anti-HIV activity, *J. Pharmaceut. Sci.* 93 (2004) 2448–2457, <https://doi.org/10.1002/jps.20156>;
 b) R.W. Dellinger, A.M. Garcia, F.L. Meyskens, Differences in the glucuronidation of resveratrol and pterostilbene: altered enzyme specificity and potential gender differences, *Drug Metabol. Pharmacokinet.* 29 (2014) 112–119, <https://doi.org/10.2133/dmpk.DMPK-13-RG-012>.
- [7] H.H.S. Chow, L.L. Garland, C.H. Hsu, D.R. Vining, W.M. Chew, J.A. Miller, M. Perloff, J.A. Crowell, D.S. Alberts, Resveratrol modulates drug- and carcinogen-metabolizing enzymes in a healthy volunteer study, *Cancer Prev. Res.* 3 (2010) 1168–1175, <https://doi.org/10.1158/1940-6207.CAPR-09-0155>.
- [8] D.C. Ferraz da Costa, F.A. Casanova, J. Quarti, M.S. Malheiros, D. Sanches, P.S. dos Santos, E. Fialho, J.L. Silva, Transient transfection of a wild-type p53 gene triggers resveratrol-induced apoptosis in cancer cells, *PLoS One* 7 (2012), e48746, <https://doi.org/10.1371/journal.pone.0048746> P53.
- [9] H.Y. Lin, H.Y. Tang, F.B. Davis, P.J. Davis, Resveratrol and apoptosis, *Ann. N. Y. Acad. Sci.* 1215 (2011) 79–88, <https://doi.org/10.1111/j.1749-6632.2010.05846>.
- [10] K.Y. Chen, C.C. Chen, Y.C. Chang, M.C. Chang, Resveratrol induced premature senescence and inhibited epithelial-mesenchymal transition of cancer cells via induction of tumor suppressor Rad9, *PLoS One* 14 (2019), e0219317, <https://doi.org/10.1371/2fjournal.pone.0219317>.
- [11] R. Pradhan, S. Chatterjee, K.C. Hembram, C. Sathy, M. Mandal, C.N. Kundu, Nano formulated resveratrol inhibits metastasis and angiogenesis by reducing inflammatory cytokines in oral cancer cells by targeting tumor associated macrophages, *J. Nutr. Biochem.* 92 (2021), 108624.
- [12] A. Bishayee, Cancer prevention and treatment with resveratrol: from rodent studies to clinical trials, *Cancer Prev. Res.* 2 (2009) 409–418, <https://doi.org/10.1158/1940-6207.capr-08-0160>.
- [13] J.E. McMurry, M.P. Fleming, New method for the reductive coupling of carbonyls to olefins. Synthesis of β -carotene, *J. Am. Chem. Soc.* 96 (1974) 4708–4709, <https://doi.org/10.1021/ja00821a076>.
- [14] a) M. Lu, B. Liu, H. Xiong, F. Wu, C. Hu, P. Liu, Trans-3,5,4'-trimethoxystilbene reduced gefitinib resistance in NSCLCs via suppressing MAPK/Akt/Bcl-2 pathway by upregulation of miR-345 and miR-498, *J. Cell Mol. Med.* 23 (2019) 2431–2441, <https://doi.org/10.1111/jcmm.14086>;
 b) F.S. Aldawsari, C.A. Velazquez-Martinez, 3,4',5-trans-Trimethoxystilbene; a natural analogue of resveratrol with enhanced anticancer potency, *Invest. N. Drugs* 33 (2015) 775–786, <https://doi.org/10.1007/s10637-015-0222-x>;
 c) D. Alex, E.C. Leong, Z.J. Zhang, Resveratrol derivative, trans-3,5,4'-trimethoxystilbene, exerts antiangiogenic and vascular-disrupting effects in zebrafish through the downregulation of VEGFR2 and cell-cycle modulation, *J. Cell. Biochem.* 109 (2010) 339–346, <https://doi.org/10.1002/jcb.22405>;
 d) M.H. Pan, J.H. Gao, Antitumor activity of 3,5,4'-trimethoxystilbene in COLO 205 cells and xenografts in SCID mice, *Mol. Carcinog.* 47 (2008) 184–196, <https://doi.org/10.1002/mc.20352>;
 e) J.H. Tsai, L.S. Hsu, C.L. Lin, 3,5,4'-Trimethoxystilbene, a natural methoxylated analog of resveratrol, inhibits breast cancer cell invasiveness by downregulation of PI3K/Akt and Wnt/beta-catenin signalling cascades and reversal of epithelial-mesenchymal transition, *Toxicol. Appl. Pharmacol.* 272 (2013) 746–756, <https://doi.org/10.1016/j.taap.2013.07.019>;
 f) Y.T. Yang, C.J. Weng, C.T. Ho, G.C. Yen, Resveratrol analog-3,5,4'-trimethoxy-trans-stilbene inhibits invasion of human lung adenocarcinoma cells by suppressing the MAPK pathway and decreasing matrix metalloproteinase-2 expression, *Mol. Nutr. Food Res.* 53 (2009) 407–416, <https://doi.org/10.1002/mnfr.200800123>.
- [15] K. Pchalek, A.W. Jones, M.M.T. Wekking, D.S.C. Black, Synthesis of activated 3-substituted indoles: an optimised one-pot procedure, *Tetrahedron* 61 (2005) 77–82, <https://doi.org/10.1016/j.tet.2004.10.060>.
- [16] J. Li, Y. Mizukami, X. Zhang, W.S. Jo, D.C. Chung, Gastroenterology 128 (2005) 1907–1918, <https://doi.org/10.1053/j.gastro.2005.02.067>.
- [17] L. Kriegl, In-situ-Analysen molekularer Mechanismen der kolorektalen Karzinogenese [In situ analyses of molecular mechanisms of colorectal carcinogenesis, *Pathologie* 34 (Suppl 2) (2013) 269–273, <https://doi.org/10.1007/s00292-013-1821-y>. German.
- [18] F. Okada, J.W. Rak, B.S. Crois, B. Lieubeau, M. Kaya, L. Roncari, S. Shirasawa, T. Sasazuki, R.S. Kerbel, Impact on oncogenes in tumor angiogenesis: mutant K-Ras up-regulation of vascular endothelial growth factor/vascular permeability factor is necessary, but not sufficient for tumorigenicity of human colorectal carcinoma cells, *Proc. Natl. Acad. Sci. USA* 95 (1998) 3609–3614, <https://doi.org/10.1073/pnas.95.7.3609>.
- [19] X. Zhang, J.P. Gaspard, D.C. Chung, Regulation of vascular endothelial growth factor by the Wnt and K-ras pathways in colonic neoplasia, *Cancer Res.* 61 (2001) 6050–6054.
- [20] a) P. García-Alfonso, E. Grande, E. Polo, R. Afonso, J.J. Reina, M. Jorge, J. M. Campos, V. Martínez, C. Ángeles, C. Montagut, The role of antiangiogenic agents in the treatment of patients with advanced colorectal cancer according to K-RAS status, *Angiogenesis* 17 (2014) 805–821, <https://doi.org/10.1007/s10456-014-9433-6>;
 b) V. Trapp, B. Parmakhtiar, V. Papazian, L. Willmott, J.P. Fruehauf, Anti-angiogenic effects of resveratrol mediated by decreased VEGF and increased TSP1 expression in melanoma-endothelial cell co-culture, *Angiogenesis* 13 (2010) 305–315, <https://doi.org/10.1007/s10456-010-9187-8>.
- [21] a) Y. Gao, M.J. van Haren, N. Buijs, P. Innocenti, Y. Zhang, D. Sartini, R. Campagna, M. Emanuelli, R.B. Parsons, W. Jespers, H. Gutiérrez-de-Terán, G.J. P. van Westen, N.I. Martin, Potent inhibition of nicotinamide N-methyltransferase by alkene-linked bisubstrate mimics bearing electron deficient aromatics, *J. Med. Chem.* 64 (2021) 12938–12963, <https://doi.org/10.1007/s00292-013-1821-y>;
 b) W. Wang, C. Yang, T. Wang, Complex roles of nicotinamide N-methyltransferase in cancer progression, *Cell Death Dis.* 267 (2022), <https://doi.org/10.1038/s41419-022-04713-z>. Open Access.
- [22] P.R. Holland, P.J. Goadsby, Targeted CGRP small molecule antagonists for acute migraine therapy, *Neurotherapeutics* 15 (2018) 304–312, <https://doi.org/10.1007/s13311-018-0617-4>.
- [23] H. Sun, D.W. Dodick, S. Silberstein, P.J. Goadsby, U. Reuter, M. Ashina, Safety and efficacy of AMG-334 for prevention of episodic migraine: a randomised, double-blind, placebo-controlled, phase 2 trial, *Lancet Neurol.* 15 (2016) 382–390, [https://doi.org/10.1016/S1474-4422\(16\)00019-3](https://doi.org/10.1016/S1474-4422(16)00019-3).
- [24] M. Morris, S. Maeda, K. Vossel, L. Mucke, The many faces of tau, *Neuron* 70 (2011) 410–426, <https://doi.org/10.1016/j.neuron.2011.04.009>.
- [25] L.R. Mueller, B. Combs, M.M. Alhadidy, S.T. Brady, G.A. Morfini, M.N. Kanaan, Tau: a signaling hub protein, *Front. Mol. Neurosci.* 14 (2021), 647054, <https://doi.org/10.3389/fnmol.2021.647054>.
- [26] T. Mosman, Rapid colorimetric assay for cellular growth and survival, application to proliferation and cytotoxicity assays, *J. Immunol. Methods* 65 (1983) 55–63, [https://doi.org/10.1016/0022-1759\(83\)90303-4](https://doi.org/10.1016/0022-1759(83)90303-4).
- [27] G.P. Carroll, S. Srivastava, A.S. Volini, M.M. Piñero-Núñez, T. Vetman, Measuring the effectiveness and impact of an open innovation platform, *Drug Discov. Today* 22 (2017) 776–785, <https://doi.org/10.1016/j.drudis.2017.01.009>.